Ultrafast dynamics of Faraday rotation in thin films

Margarita I. Sharipova, Alexander I. Musorin, Tatyana V. Dolgova, and Andrey A. Fedyanin

Faculty of Physics, Lomonosov Moscow State University, Moscow 119991, Russia

ABSTRACT

Femtosecond Faraday rotation evolution and a propagation of a femtosecond pulse through a thin magnetic films is calculated and measured.

Keywords: Faraday effect, gyrotropic media, femtosecond processes, polarization control

1. INTRODUCTION

Photonic crystals are key elements of the all-optical devices concept providing a mechanism to control and manipulate the flow of light. The embedding one or more magnetic layer leads to enhancement of magneto-optical response of magnetophotonic crystal because of concentration of the light in magnetic media.[1] These optical cavities are attractive for optical communication system, spatial light modulators, holographic memory, etc.[2,3] The simplest case of optical cavity is a thin magnetic film. The magneto-optical signal in layered magnetic samples is proportional to the thickness of the film and to the contrast of reflection indices of the film and the environment. Various time-resolved techniques are used to study magnetization dynamics of a system perturbed by a powerful femtosecond laser pulse.[4,5] The evolution of light polarization within a single femtosecond pulse in an unperturbed system is determined by a relation time duration of the pulse and traverse time of the pulse inside a sample. If the duration is greater than traverse time,[6] then the polarization rotation shouldn't be large because of small light-matter interaction time. On the contrary, if the traverse time is greater than duration of the pulse, then light polarization evolution is more complex.

In this work, femtosecond Faraday rotation evolution and a propagation of a femtosecond pulse through thin magnetic films is calculated and measured.

2. THEORY

2.1 Multiple Interference of monochromatic light in the Faraday-active Fabry-Perot etalon

Suppose a monochromatic plane wave propagates in vacuum and goes through the parallel-sided plate with angle of incidence equals to α. The electromagnetic field of the wave can be written as

$$\vec{E}_0 = \vec{A}_0 e^{i(\vec{k}\vec{r}-\omega t)},\ \vec{A}_0 = A_0 \begin{pmatrix} 1 \\ 0 \end{pmatrix}, \tag{1}$$

If we neglect absorption, then we can describe optical properties of the plate, using just a few parameters: plate's thickness d, its refractive index n, reflectance and transmittance field amplitude at the plate's border indices ρ and τ, respectively. The connection between the parameters is following:

$$R = \rho^2; T = \tau^2, R + T = 1, \tag{2}$$

$$\sin\alpha = n \sin\beta, \tag{3}$$

$$\delta = 2\frac{\omega}{c} dn \cos\beta, \tag{4}$$

E-mail: sharipova@nanolab.phys.msu.ru

Metamaterials X, edited by Vladimír Kuzmiak, Peter Markos, Tomasz Szoplik, Proc. of SPIE
Vol. 9502, 95020O · © 2015 SPIE · CCC code: 0277-786X/15/$18 · doi: 10.1117/12.2180635

where R, T — reflectance and transmittance of the light intensity at the borders, β — angle of refraction, c — speed of light and δ — phase difference between the transmitted light and light, which was reflected twice inside the plate from its borders borders and came out. The resulting output light can be written as

$$\vec{E} = \vec{E}_0\tau^2(1 + \rho^2 e^{i\delta} + \rho^4 e^{2i\delta} + ...) = \vec{E}_0\tau^2 \sum_{m=0}^{\infty} (\rho^2 e^{i\delta})^m. \tag{5}$$

After summing up:

$$\vec{E} = \vec{E}_0 \frac{\tau^2}{1 - \rho^2 e^{i\delta}}. \tag{6}$$

The total transmittance $T(\delta) = I/I_0$ equals to:

$$T(\delta) = \frac{T^2}{|1 - Re^{i\delta}|^2};$$

or, in the real numbers:

$$T(\delta) = \frac{1}{1 + F\sin^2(\frac{\delta}{2})}, \tag{7}$$

where F — factor of sharpness. The formula was derived for the first time by Airy.[7]

$$F = \frac{4R}{(1 - R)^2}. \tag{8}$$

Fig. 1 shows transmittance T versus phase difference δ with different values of F. The factor of sharpness defines a magnitude of the oscillations according to Eq. (7): the more is the value of F, the bigger becomes the amplitude of oscillation.

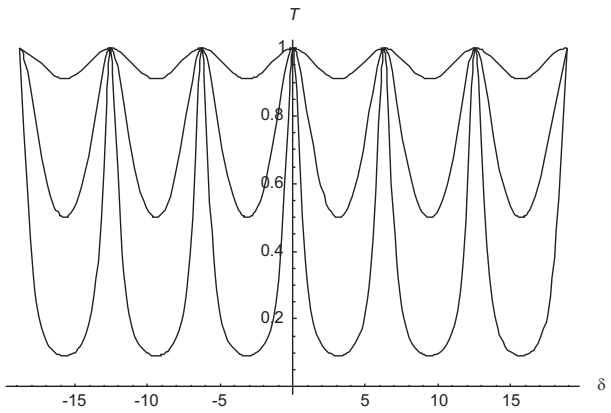

Figure 1. Transmittance T versus phase difference δ with different F values. From top to bottom: $F = 0.1; 1; 10$.

In gyrotropic materials, such as Faraday-active media, the rotation of polarization plane will also be different in each component:

$$\vec{E} = A_0\tau^2 \left(\begin{pmatrix} \cos\theta \\ \sin\theta \end{pmatrix} + \rho^2 e^{i\delta} \begin{pmatrix} \cos 3\theta \\ \sin 3\theta \end{pmatrix} + \rho^4 e^{2i\delta} \begin{pmatrix} \cos 5\theta \\ \cos 5\theta \end{pmatrix} + ... \right); \tag{9}$$

where θ is a Faraday rotation of the light after going trough the gyrotropic media with thickness d. Consequently, the Faraday rotation is equal 2θ for light returned to origin after reflection from far border due to the non-reciprocity of the effect. It's easier to work in exponential notation:

$$\vec{E} = A_0\tau^2 \left(\begin{pmatrix} \frac{e^{i\theta}+e^{-i\theta}}{2} \\ \frac{e^{i\theta}-e^{-i\theta}}{2i} \end{pmatrix} + \rho^2 e^{i\delta} \begin{pmatrix} \frac{e^{i3\theta}+e^{-i3\theta}}{2} \\ \frac{e^{i3\theta}-e^{-i3\theta}}{2i} \end{pmatrix} + \rho^4 e^{2i\delta} \begin{pmatrix} \frac{e^{i5\theta}+e^{-i5\theta}}{2} \\ \frac{e^{i5\theta}-e^{-i5\theta}}{2i} \end{pmatrix} + ... \right); \tag{10}$$

$$\Downarrow$$

$$\vec{E} = A_0\tau^2 \sum_{m=0}^{\infty} (\rho^2 e^{i\delta})^m \begin{pmatrix} \frac{e^{i\theta(2m+1)}+e^{-i\theta(2m+1)}}{2} \\ \frac{e^{i\theta(2m+1)}-e^{-i\theta(2m+1)}}{2i} \end{pmatrix}. \tag{11}$$

As a result, one should sum up two projections separately:

$$\vec{E} = A_0\tau^2 \begin{pmatrix} \frac{e^{i\theta}}{2} \sum\limits_m (\rho^2 e^{i\delta+i2\theta})^m + \frac{e^{-i\theta}}{2} \sum\limits_m (\rho^2 e^{i\delta-i2\theta})^m \\ \frac{e^{i\theta}}{2i} \sum\limits_m (\rho^2 e^{i\delta+i2\theta})^m - \frac{e^{-i\theta}}{2i} \sum\limits_m (\rho^2 e^{i\delta-i2\theta})^m \end{pmatrix}; \tag{12}$$

$$\vec{E} = A_0\tau^2 \begin{pmatrix} \frac{1}{2}\left(\frac{e^{i\theta}}{1-\rho^2 e^{i2\theta+i\delta}} + \frac{e^{-i\theta}}{1-\rho^2 e^{-i2\theta+i\delta}}\right) \\ \frac{1}{2i}\left(\frac{e^{i\theta}}{1-\rho^2 e^{i2\theta+i\delta}} - \frac{e^{-i\theta}}{1-\rho^2 e^{-i2\theta+i\delta}}\right) \end{pmatrix}; \tag{13}$$

$$\vec{E} = \frac{A_0\tau^2}{1+\rho^4 e^{2\imath\delta} - 2\rho^2 e^{\imath\delta}\cos 2\theta} \begin{pmatrix} (1-\rho^2 e^{\imath\delta})\cos\theta \\ (1+\rho^2 e^{\imath\delta})\sin\theta \end{pmatrix}. \tag{14}$$

Amplitude of the transmitted electric field:

$$|\vec{E}| = A_0\tau^2 \begin{pmatrix} \sqrt{\frac{1-2\rho^2\cos\delta+\rho^4}{1-4\rho^2\cos\delta\cos 2\theta+2\rho^4\cos 2\delta-4\rho^4\cos^2 2\theta-4\rho^6\cos\delta\cos 2\theta+\rho^8}}\cos\theta \\ \sqrt{\frac{1+2\rho^2\cos\delta+\rho^4}{1-4\rho^2\cos\delta\cos 2\theta+2\rho^4\cos 2\delta-4\rho^4\cos^2 2\theta-4\rho^6\cos\delta\cos 2\theta+\rho^8}}\sin\theta \end{pmatrix}. \tag{15}$$

After normalizing the Jones vector of polarization

$$|\vec{E}| = A_0\tau^2 \sqrt{\frac{1-2\rho^2\cos\delta\cos 2\theta+\rho^4}{(1-2\rho^2\cos(\delta+2\theta)+\rho^4)(1-2\rho^2\cos(\delta-2\theta)+\rho^4)}} \begin{pmatrix} \frac{\cos\theta}{\sqrt{1+\frac{4\rho^2\cos\delta\sin^2\theta}{1-2\rho^2\cos\delta\cos 2\theta+\rho^4}}} \\ \frac{\sin\theta}{\sqrt{1+\frac{4\rho^2\cos\delta\cos^2\theta}{1-2\rho^2\cos\delta\cos 2\theta+\rho^4}}} \end{pmatrix}. \tag{16}$$

Now we can write the resulting transmittance T^{output} and total Faraday rotation Φ:

$$T^{output} = \frac{(1-R)^2(1-2R\cos\delta\cos 2\theta+R^2)}{(1-2R\cos(\delta+2\theta)+R^2)(1-2R\cos(\delta-2\theta)+R^2)}; \tag{17}$$

$$\Phi(R,\theta,\delta) = \arctan\left(\sqrt{1+\frac{4R\cos\delta}{1-2R\cos\delta+R^2}}\tan\theta\right). \tag{18}$$

In the case of $\theta \to 0$, T^{output} turns into T.

Fig. 2 shows interference pattern of Faraday rotation. Without interference Faraday rotation equals to 0.02 radians, but in the presence of interference it varies from zero to 0.2 radians.

Fig. 3 shows transmittance T and Faraday rotation Φ. The transmittance maxima coincide with maxima of Faraday rotation.

The more complicated analysis, taking into account magnetic circular dichroism, has been previously done.[8] As we are mostly interested in pure Faraday effect studied in pulsed light, we decided to neglect arising ellipticity. In the experiment the evaluated ellipticity was not greater than 10^{-5}.

2.2 Multiple interference of pulsed light in the Faraday-active Fabry-Perot etalon

Suppose a single light pulse with a gaussian shape propagates through a gyrotropic medium. The incoming electromagnetic field can be written as

$$\vec{E}_0(t) = \vec{A}_0 e^{-(\omega_0 t)^2}, \vec{A}_0 = A_0 \begin{pmatrix} 1 \\ 0 \end{pmatrix}. \tag{19}$$

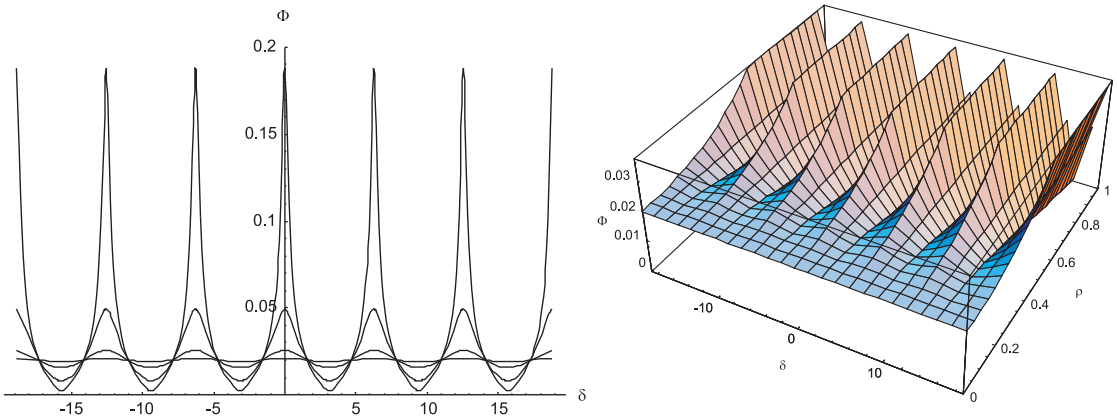

Figure 2. (Color online)**left**: Several subsection of Faraday oscillations for $\theta = 0.02$ and $\rho = 0.15; 0.35; 0.65; 0.9$. **right**: Faraday oscillations for $\theta = 0.02$.

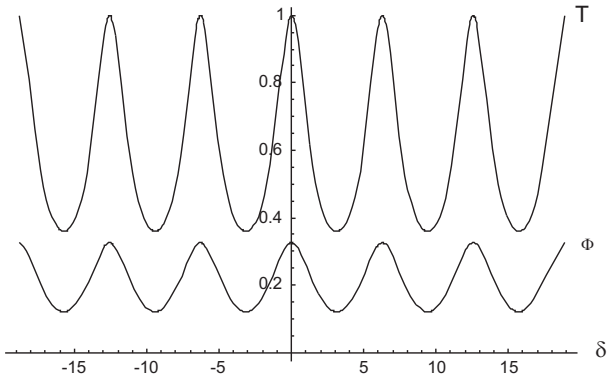

Figure 3. Interference pattern of transmittance T and Faraday rotation Φ when $\theta = 0.2$ radian and $\rho = 0.5$.

where $\omega_0 = 1/\tau_0$, and τ_0 is a pulse duration. Then the output signal will be the sum of the pulses, repeatedly reflected inside the film. The polarization of each reflection will be proportional to the distance passed inside the media:

$$\vec{E} = A_0\tau^2 \left(e^{-(\omega_0 t)^2} \begin{pmatrix} \cos\theta \\ \sin\theta \end{pmatrix} + \rho^2 e^{i\delta} e^{-(\omega_0(t-\Delta))^2} \begin{pmatrix} \cos 3\theta \\ \sin 3\theta \end{pmatrix} + \rho^4 e^{i2\delta} e^{-(\omega_0(t-2\Delta))^2} \begin{pmatrix} \cos 5\theta \\ \sin 5\theta \end{pmatrix} + ... \right), \quad (20)$$

where $\Delta = 2nd/c$, and equals to the time delay between the first transmitted pulse and its second replica reflected inside the film. In the latter expression we denoted zero time $t = 0$ for the moment when maximum of the transmitted pulse comes out of the plate.

$$\vec{E} = A_0\tau^2 \sum_{m=0}^{\infty} e^{-(\omega_0(t-m\Delta))^2} (\rho^2 e^{i\delta})^m \begin{pmatrix} \cos\ (2m+1)\theta \\ \sin\ (2m+1)\theta \end{pmatrix}. \quad (21)$$

Then the resulting Faraday Φ rotation will be:

$$\Phi = \arctan \left(\frac{\sum\limits_m e^{-(\omega_0(t-m\Delta))^2} (\rho^2 e^{i\delta})^m \ \sin(2m+1)\theta}{\sum\limits_m e^{-(\omega_0(t-m\Delta))^2} (\rho^2 e^{i\delta})^m \ \cos(2m+1)\theta} \right). \quad (22)$$

The control parameter in this expression is $\omega_0\Delta$ — that combination is the ratio between time which light spends inside the film Δ and pulse duration τ_0.

The expression (22) holds absolute convergeness, as majorized by harmonic geometric progression. However, there is no simplification for these series. In order to analyze the results, let us consider three cases with different values of operating parameters.

1. Case $\omega_0\Delta \ll 1$.

   This inequality holds true when the time of pulse transmitting through the film is much shorter than the pulse duration, i.e., the steady-state case. For that we can neglect small changes in index of exponential part:

$$e^{-(\omega_0(t-m\Delta))^2} = e^{-(\omega_0 t - m\omega_0\Delta)^2)} \approx e^{-(\omega_0 t)^2}. \tag{23}$$

   Consequently, we may take the exponent out of the sum in equation (22):

$$\Phi = \arctan\left(\frac{e^{-(\omega_0 t)^2}\sum\limits_m(\rho^2 e^{i\delta})^m \ \sin(2m+1)\theta}{e^{-(\omega_0 t)^2}\sum\limits_m(\rho^2 e^{i\delta})^m \ \cos(2m+1)\theta}\right) = \arctan\left(\frac{\sum\limits_m(\rho^2 e^{i\delta})^m \ \sin(2m+1)\theta}{\sum\limits_m(\rho^2 e^{i\delta})^m \ \cos(2m+1)\theta}\right) = \Phi(R,\theta,\delta). \tag{24}$$

   As we might anticipate, the resulting Faraday rotation does not depend on time. We see that this case comes to the previous subsection of steady-state Faraday rotation (see expression (18)).

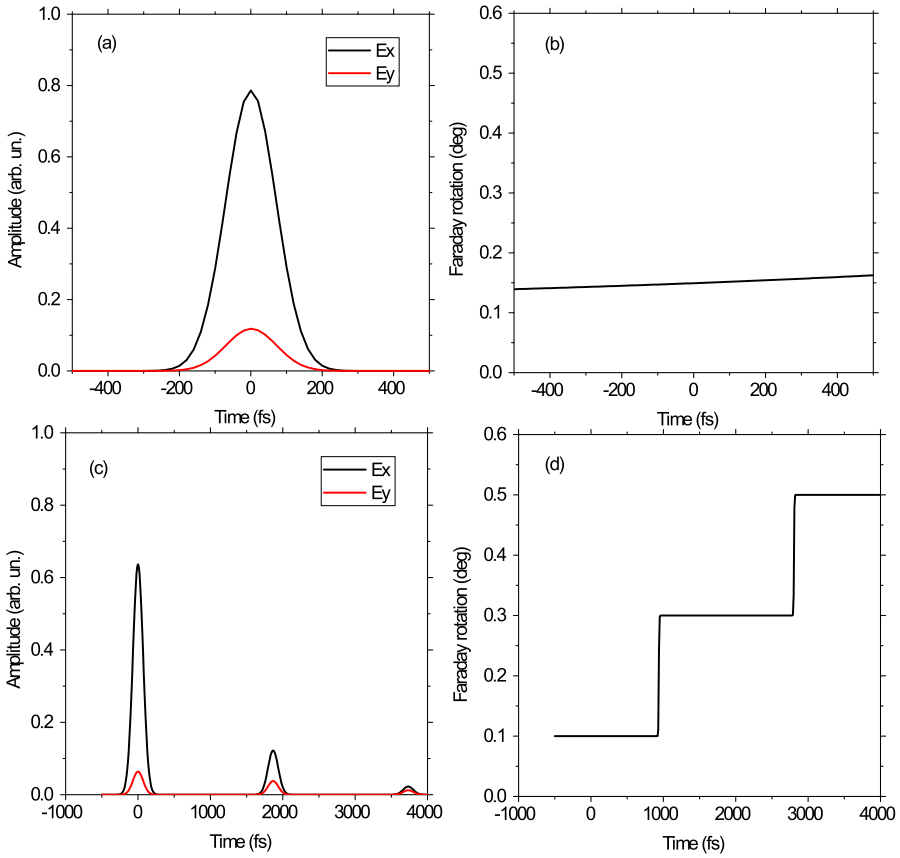

Figure 4. (Color online) (a) and (c) Projections E_x, E_y versus time. (b) and (d) Faraday rotation versus time. $\theta = 0.1$ radian, $\rho = 0.2$. (a) and (b) corresponds to $\omega_0\Delta \ll 1$ case. (c) and (d) corresponds to $\omega_0\Delta \gg 1$ case.

Fig. 4 (a,b) shows calculated projections E_x, E_y and Faraday rotation versus time. We have summed first 150 components in the expression (22). The values of the parameters were: $\tau_0 = 100$ fs, $\Rightarrow \omega_0 = 10^{13}$ $1/s$,

$\Delta = 2$ fs, $\rho = 0.2$, and $\theta = 0.1$ radian. As was expected, the output pulse is gaussian. Faraday rotation is constant.

2. Case $\omega_0 \Delta \gg 1$.

   This inequality means that subsequent replicas do not overlap in time. This is correct in case of thick material and short pulse. As each component is independent and does not sum with each other, it is possible to remove the sum sign. In this assumption we can simplify the expression (22) for Φ, as we might neglect all components of sum except one in a given time interval:

$$\text{if } t \in [\Delta(\widetilde{m} - \frac{1}{2}, \widetilde{m} + \frac{1}{2})], \text{ then } \sum_m e^{-(\omega_0(t-m\Delta))^2} f(m) \approx e^{-(\omega_0(t-\widetilde{m}\Delta))^2} f(\widetilde{m}) \tag{25}$$

   We should keep in mind that the sum index m and time t are related. We can now calculate the output:

$$\Phi(t) \approx \sum_m \arctan\left(\frac{e^{-(\omega_0(t-m\Delta))^2}\rho^{2m}\ \sin(2m+1)\theta}{e^{-(\omega_0(t-m\Delta))^2}\rho^{2m}\ \cos(2m+1)\theta}\right); \tag{26}$$

$$\Phi(t) = \arctan\left(\frac{\sin(2m+1)\theta}{\cos(2m+1)\theta}\right) = ((2m+1)\theta); \tag{27}$$

   where sum index $m = \left[\frac{t}{\Delta}\right] + 1$ and defined by how many pulse replicas were transmitted through the sample at that time.

   Fig. 4 (c,d) shows calculated projections E_x, E_y and Faraday rotation versus time. We have summed first 150 components in the expression (22). The values of the parameters were: $\tau_0 = 100$ fs, $\Rightarrow \omega_0 = 10^{13}\ 1/s$, $\Delta = 2000$ fs, $\rho = 0.2$, and $\theta = 0.1$ radian. The Faraday rotation evolution is a step-like function. Electric field profile is a number of pulse replicas with gaussian line shapes. The magnitude of a replica x field component decreases with time due to transversion to y component as well as reflection and transmission components. Simultaneously magnitude of y field component of each replica decreases due to reflection and transmission components as well as x field component but increases due to polarization rotation.

3. Case $\omega_0 \Delta \sim 1$.

   This case happens when pulse duration is comparable with the in-plate propagation time. In that condition there is a significant influence of interference effects. However, this case is hard to analyse, as there is no components on Eq. 22, which we can neglect. Thus, it is hard to give even qualitative assesment.

3. NUMERICAL CALCULATIONS OF FEMTOSECOND FARADAY ROTATION AND PULSE EVOLUTION IN THIN FILMS

As was previously mentioned, we have got expression (22) for Faraday rotation of pulsed light while using several simplifications. We have worked in linear basis, though the symmetry of the problem suggests circular basis. As a result, we didn't take into account the difference of coefficients ρ, τ for left- and right- circularly polarized light. Though this is not critical, we have decided to check the theory by performing numerical simulations. In addition, theoretical approach will be inapplicable in case of more complex structures, such as photonic crystals.[9]

The calculations of Faraday rotation dynamics and a femtosecond pulse propagation through a thin magnetic film were made by the 4x4 transfer-matrix formalism and the fast Fourier transformation. The permittivity tensor of the sample is non-dispersive:

$$\hat{\varepsilon} = \begin{pmatrix} 7.84 & -0.0055i & 0 \\ 0.0055i & 7.84 & 0 \\ 0 & 0 & 7.84 \end{pmatrix}. \tag{28}$$

A spatial length of the pulse has been fixed $L = 45\ \mu m$. It corresponds to time duration of the pulse of 150 fs. We have varied the film thickness d as in Sec. 2. Three cases of relation between L and nd have been studied: $L >> nd$, $L \sim nd$, $L << nd$.

The time evolution of a single femtosecond pulse which has passed through the sample is shown on Fig. 5 (a). The zero time corresponds to the moment when maximum pulse intensity reaches the second border of the structure, while inferred film with refractive index $n = 1$. Let the light enter the film at the interface '1' and exit at the interface '2'.

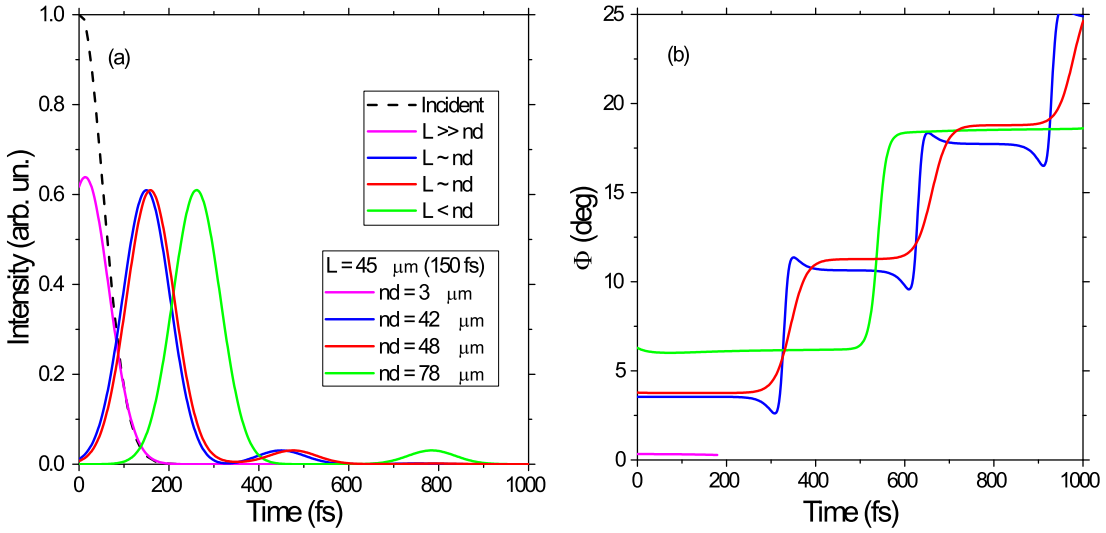

Figure 5. (Color online) The result of numerical simulation of a single femtosecond pulse propagation through a thin magnetic film (a) and a femtosecond polarization rotation evolution for three cases of ratio between the spatial pulse duration L and the sample's optical thickness nd. A dash line is an envelope of incoming pulse. The pink line corresponds to $L >> nd$ case, blue and red — $L \sim nd$, the green line — $L < nd$.

Let us describe the case $L < nd$ (Fig. 5 (a), a green line). The maximum of the first transmitted part of the pulse reaches the interface '2' at 260 fs. Maximum of the double reflected in the film pulse exits at 780 fs. The time difference between the first and second transmitted pulses is approximately 500 fs and "tails" overlapping can be neglected.

In the case $L \sim nd$ (see Fig. 5 (a), blue and red lines) the maxima of the pulses come at the time ∼150 fs and ∼440 fs. In this case "tails" are overlapping in time. And interference effects can be found in overlapping area depending on the phase relation between the pulse parts.

In the case $L >> nd$ (see Fig. 5 (a), pink line) the pulse passes through the film almost like a steady-state signal. Numerical simulation of the Faraday rotation evolution (pink line) for this case is shown in Fig. 5 (b). These results correspond well with the theory (for comparison see Fig. 4).

In the case $L \sim nd$ (see Fig.5 (b), blue line) there is an area with negative time derivative. It can be explained by destructive interference of transmitted part pulse "tail" and double reflected one. But for the same case $L \sim nd$ a positive derivative is also possible (see fig. 5 (b), a red line), when the interference of the pulses is constructive.

In the case $L < nd$ the Faraday rotation time dependence (see Fig.5 (b), green line) is a step-like function because the "tails" don't overlap. The value of the step is three time larger than initial polarization rotation due to triple optical path of double reflected part of the pulse.

Let us explain the effect qualitatively (see Fig.6 (**left**)). Let the light propagates in Z direction through the film placed in xOy plane. The plane xOy in Fig. 6 (**left**) is an the interface '2'. Let the electric field of the once transmitted pulse $\vec{E}_1$ is under Faraday rotation θ_1 to axis Y. After two reflections inside the film a phase of the electric field $\vec{E}_{2A}$ is close to the phase of transmitted pulse $\vec{E}_1$. Polarization rotation of double reflected pulse $\vec{E}_{2A}$ is θ_{2A}. And "tails" are overlapped. Then superposition $\vec{E}_A$of electric fields is rotated under θ_A. I.e. in first

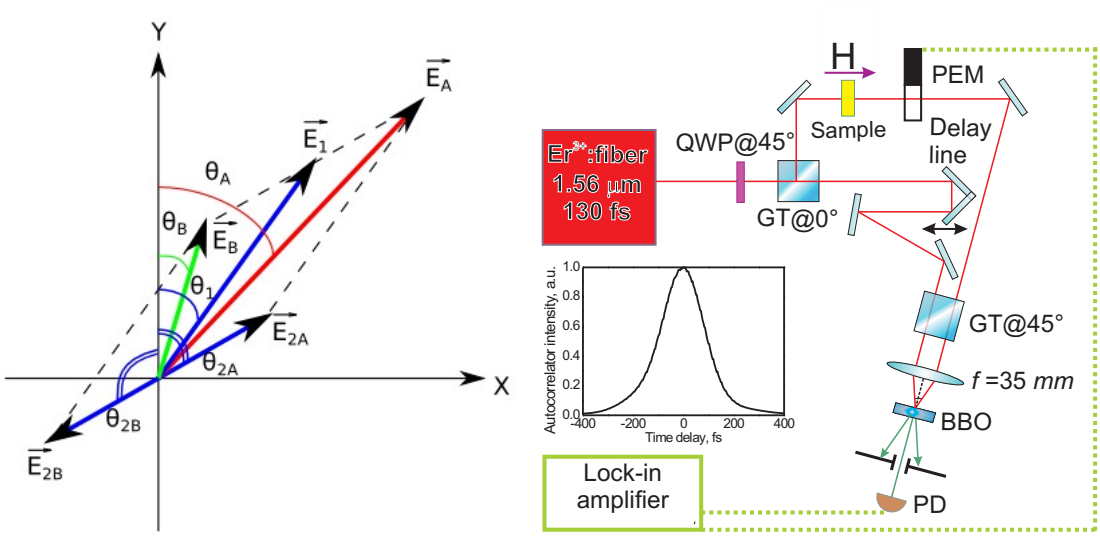

Figure 6. (Color online) **left**: Scheme of electric fields superposition of transmitted and double reflected parts of the pulse propagated through the film. Blue arrows — electric fields of the pulse parts, a red arrow — superposition of fields in constructive interference case, a green arrow — in case of destructive interference. **right**: Experimental setup. Input pulse goes into Glan-Taylor prism, which works as polarization beam splitter and divides into signal and reference pulses. Reference pulse goes through a variable delay line and signal pulse goes through a sample placed in magnetic field. If the sample is Faraday-active, then vertical polarization component of the signal pulse is modulated at the double PEM frequency. Autocorrelation function of the input pulse is shown in the center of the figure, it has gaussian line shape.

part of the pulse the rotation is θ_1, at overlapped moment — $\theta_A > \theta_1$ and in second part is $\theta_{2A} > \theta_A > \theta_1$. Thus, Faraday rotation is increasing with time due to constructive interference.

If the phase of double reflected pulse is opposite to the transmitted one, the electric field $\vec{E}_{2B}$ is under Faraday rotation θ_{2B}. I.e. in first part of the pulse the polarization rotation is θ_1, in the second part of the pulse the rotation is $\theta_{2B} > \theta_1$. Superposition of electric fields of the pulses in overlapped area gives an electric field under Faraday rotation θ_B. So the polarization θ_B is less than θ_1 as well as θ_{2B}. Thus, Faraday rotation is decreasing with time due to destructive interference in overlapped area.

To sum up, in case $L \sim nd$ the behavior of Faraday rotation time evolution (increasing or decreasing with time) depends on multiple reflection interference: it increases with time for constructive interference and decreases with time for destructive interference.

4. EXPERIMENTAL

Figure 6 (**right**) shows principal scheme of the experimental set-up. It is based on a modified correlation technique[10] combined with polarization-sensitive part, which uses photoelastic modulator.[11] Horizontally polarized pulses go out of an infrared femtosecond laser with following parameters: 1.56-μm wavelength, 130-fs pulse duration 70-MHz repetition rate and 140-mW average intensity. The pulse electromagnetic field can be written as

$$\vec{E}(t) = E_0(t) \begin{pmatrix} 1 \\ 0 \end{pmatrix};$$

When quarter-wave plate is rotated on 45° relative to the incoming pulse polarization, the resulting wave will be circular:

$$\vec{E}(t) = E_0(t) \frac{1}{\sqrt{2}} \begin{pmatrix} 1 \\ \imath \end{pmatrix};$$

Due to quarter-wave plate Glan prism divides input beam into two beamlets: signal pulse with vertical polarization and reference pulse with horizontal one. The reference pulse goes through a variable delay line, which

causes time delay τ:

$$\vec{E}_{ref}(t) = \frac{E_0(t-\tau)}{2}\frac{1}{\sqrt{2}}\begin{pmatrix} 0 \\ 1 \end{pmatrix};$$

The electric field of signal pulse is

$$\vec{E}_s(t) = \frac{E_0(t)}{2}\frac{1}{\sqrt{2}}\begin{pmatrix} 1 \\ 0 \end{pmatrix};$$

Signal pulse goes through the sample at normal incidence. The sample is placed in a 1-kOe static magnetic field, which is oriented parallel to the wave vector of light. After passing the sample the polarization of signal pulse differs from vertical polarization — it is rotated at the angle $\Phi(t)$:

$$\vec{E}_s(t) = \frac{E_0(t)}{2}\frac{1}{\sqrt{2}}\tilde{T}(t)\begin{pmatrix} \cos\Phi(t) \\ \sin\Phi(t) \end{pmatrix}.$$

The shape of the pulse has also been changed, which is expressed by the insertion of parameter $\tilde{T}(t)$. In this equation we neglected ellipticity of the pulse. Usually, the magnitude of the effect is rather small: $\Phi \ll 1$. Vertical component of light then becomes modulated by HINDS photoelastic modulator (PEM) with vertically oriented optical axis and eigenfrequency $f = 47$ kHz, which periodically changes delay between x and y components of the electric field in optical wave:

$$\vec{E}_s(t) = \frac{E_0(t)}{2}\frac{1}{\sqrt{2}}\tilde{T}(t)\begin{pmatrix} \cos\Phi(t)e^{A\cos(2\pi ft)} \\ \sin\Phi(t) \end{pmatrix},$$

where A — retardation amplitude of the photoelastic modulator. In the experiment $A = 2.405$ due to the special considerations mentioned below. After being reflected from several mirrors both pulses with mutually perpendicular orientations become parallel. The polarization orientation of the pulses becomes the same after going through the 45°-oriented second Glan prism:

$$\vec{E}_s(t) = \frac{E_0(t)}{2\sqrt{2}}\frac{\tilde{T}(t)}{\sqrt{2}}\begin{pmatrix} \cos\Phi(t)e^{\iota A\cos(2\pi ft)} + \sin\Phi(t) \\ \cos\Phi(t)e^{\iota A\cos(2\pi ft)} + \sin\Phi(t) \end{pmatrix};$$

$$\vec{E}_{ref}(t-\tau) = \frac{E_0(t-\tau)}{2\sqrt{2}}\frac{1}{\sqrt{2}}\begin{pmatrix} 1 \\ 1 \end{pmatrix}.$$

Both pulses are then focused at the same spot on non-linear 500-nm-thick BBO crystal by a 50-mm convex lens. If the time delay between two pulses is not very big, then they overlap and generate non-collinear second-harmonic in the direction of bisector:

$$\vec{E}_{SHG}(t) \propto \vec{E}_s(t)\vec{E}_{ref}(t-\tau) = \frac{E_0(t)E_0(t-\tau)}{16}\tilde{T}(t)\begin{pmatrix} \cos\Phi(t)e^{\iota A\cos(2\pi ft)} + \sin\Phi(t) \\ \cos\Phi(t)e^{\iota A\cos(2\pi ft)} + \sin\Phi(t) \end{pmatrix}.$$

Blue filters don't pass scattered pumping and the aperture cuts non-useful signal from collinear second harmonics. Thus, the resulting intensity is

$$I_{SHG}(t) \propto |\vec{E}_s(t)\vec{E}_{ref}(t-\tau)|^2 = \left(\frac{E_0(t)E_0(t-\tau)}{16}\right)^2 2T(t)\{1+\cos(A\cos(2\pi ft))\sin 2\Phi(t)\}.$$

where $T(t)$ reflects the difference in the intensity temporal profile. A signal collected by photodiode integrates I_{SHG} in the time domain:

$$u(\tau) = \int_{-\infty}^{\infty}\left(\frac{E_0(t)E_0(t-\tau)}{16}\right)^2 2T(t)\{1+\cos(A\cos(2\pi ft))\sin 2\Phi(t)\}dt =$$

$$= \int I_0(t, t-\tau)\{1+\cos(A\cos(2\pi ft))\sin 2\Phi(t)\}dt.$$

The time limits are $(-\infty;\infty)$, but in the experiment it shrinks to time interval $\approx 10^{-12}$ s where both pulses have non-zero intensity. Using Jacobi-Anger expansion:

$$\cos(A\cos(2\pi ft)) = \Re\{e^{A\cos 2\pi ft}\} = J_0(A_0) + 2\Re\{\sum_{n=1}^{\infty} \iota^n J_n(A_0)\cos(2n\pi ft)\} =$$

$$= J_0(A_0) + 2\sum_{n=1}^{\infty}(-1)^n J_{2n}(A_0)\cos(4n\pi ft).$$

Leaving only two summands in the expansion (supposing that high orders of sum are negligible) and putting selected retardation $A_0 = 2.405$ (due to the fact that $J_0(A_0) = 0$), we get

$$\cos(A\cos(2\pi ft)) = J_0(A_0) - 2J_2(A_0)\cos(4\pi ft)|_{A_0=2.405} = -2J_2(2.405)\cos(4\pi ft) \approx 0.86\cos(4\pi ft).$$

Thus, the detected signal consists of two components — *dc* one and high-frequency addon:

$$u(\tau) = \int I_0(t, t-\tau)\{1 - 0.86\cos(4\pi ft)\sin 2\Phi(t)\}dt$$

As PEM period of oscillation $1/f \approx 10^{-5}$s is much bigger than the time of integration ($\approx 10^{-12}$ s, comparable with pulse duration — 130 fs), then $\cos(4\pi ft) \approx const = \cos(4\pi f\bar{t})$ during the integration time and can be factored out of the integral:

$$u(\tau) \approx \int I_0(t, t-\tau)dt - 0.86\cos(4\pi f\bar{t}) \int I_0(t, t-\tau)\sin 2\Phi(t)dt = u_{dc}(\tau) + u_{2f}(\tau).$$

The measurement by the lock-in amplifier of these two components gives us a possibility to reconstruct the time dependence of Faraday rotation $\Phi(t)$. It's ratio gives us

$$\tilde{\Phi}(\tau) = \frac{1}{2}\left|\frac{u_{2f}(\tau)}{0.86u_{dc}(\tau)}\right|,$$

The equation is correct in the assumption of $\sin 2\Phi \approx 2\Phi \ll 1$. $\tilde{\Phi}(\tau)$ is an averaged magnitude of Faraday effect. The slower the changes in Faraday effect — the closer $\tilde{\Phi}$ comes to Φ. When there is no time dependence of Faraday effect at all, e.g. $\Phi(t) = const$, then the shapes of measured correlation functions $u_{dc}(\tau), u_{2f}(\tau)$ are the same. If Faraday rotation dynamics exists, then $\tilde{\Phi} \neq const$ and lineshapes of $u_{dc}(\tau), u_{2f}(\tau)$ differ from each other.

The experiment has been done for the simplest case of a layered structure — the thin magnetic film. Two films with thicknesses of 11 ($\omega_0\Delta = 0.5 < 1$) and 30 μm ($\omega_0\Delta = 1.4 \approx 1$) on gadolinium-galium garnet substrate were used. For the 11-μm film the ratio of pulse duration to the time for transmitting through the film is relatively big — so the pulse seems to be the same as in quasi-steady state. Consequently, correlation functions measured for this case have the same gaussian line shape, just as autocorrelation function.

Figure 7 demonstrates extracted from experimental data Faraday rotation evolution $\tilde{\Phi}(\tau)$, which for this case equals Φ, as there is no dynamics of Faraday rotation in 11-μm thick film. The zero time corresponds to the maximum of correlation function.

The same 11-μm thick film was used for the measurements in case $\omega\Delta \ll 1$ of the ratio of pulse duration to the time for transmitting through the film is relatively small. To achieve this case the effective thickness was a sum of film and substrate thicknesses. The measurement of such composite structure allowed us to detect the second pulse rescattered inside the sample. Figure 7 shows obtained time-resolved Faraday rotation with first and second steps of case $\omega_0\Delta = 50 \gg 1$. Its values differ in three times $\approx 1^\circ$ and $\approx 3^\circ$, which coincides with the theory and calculations.

Figure 8 shows measured correlation functions at chopper and double PEM frequencies for the 30 μm-thick-film. On both graphs a small shoulder at the right side of the correlation function is seen. These peculiarities appear at the time 400 fs. The difference of correlation function from gaussian shape shows that Faraday rotation is not contant. Though to extract direct dependence we had to make additional experiments and alter the experimental setup.[12]

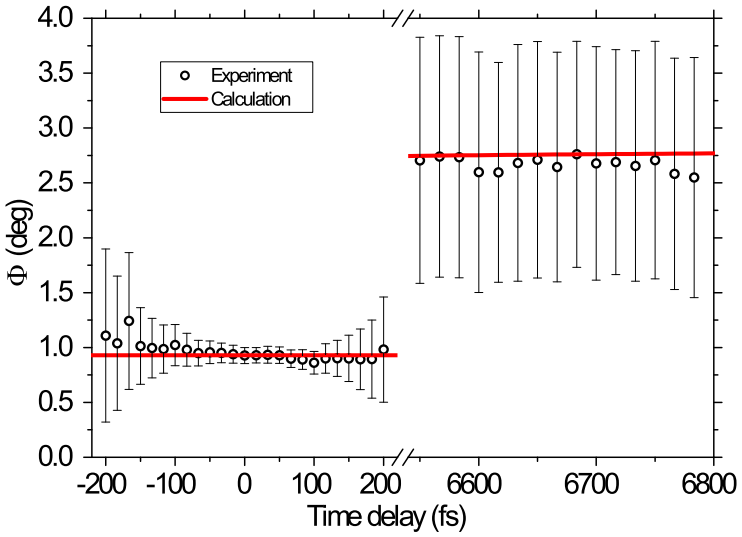

Figure 7. (Color online) Femtosecond Faraday rotation evolution of a pulse transmitted through a 11-μm-thick film. Dots — experimental results, line — calculations. At the times smaller than 200 fs the quasi-steady-state case $\omega_0\Delta \ll 1$ is applicable, at the times up to 6800 fs the case of thick film $\omega_0\Delta \gg 1$ takes place.

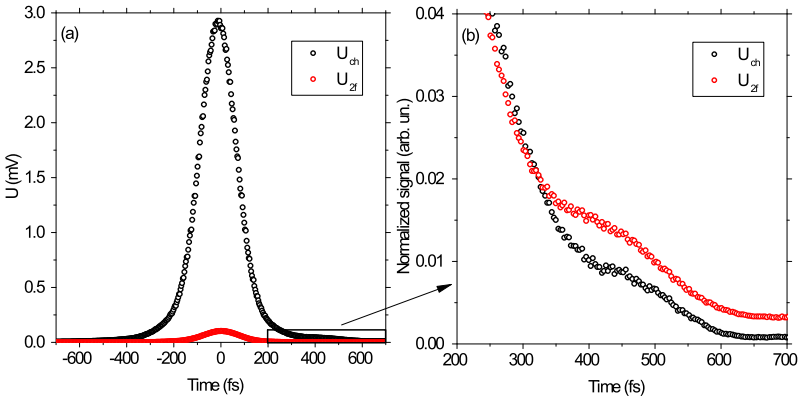

Figure 8. (Color online)(a) Correlation functions of a reference pulse and a signal pulse transmitted through a 30-μm-thick film measured at the chopper frequency (black dots) and at the double PEM frequency 2f (red dots). (b) Zoom of 200-700 fs range of normalized correlation functions.

5. CONCLUSION

Femtosecond time dependence of Faraday rotation in magnetic films has been studied theoretically, numerically and experimentally. We have separated three general cases: the film traversal time is less, greater and comparable than the pulse duration. The first one is similar to steady-state case. There is no time dependence of Faraday rotation. Faraday rotation is a step-like function of time for the second case. In the last case Faraday rotation time evolution is strongly depends on the interference conditions. This withdrawal allows one to expect well-controlled and stronger effects in high Q-factor structured materials, such as photonic crystals.

ACKNOWLEDGMENTS

This work was supported in part by the Russian Foundation for Basic Research and Ministry of Education and Science of Russian Federation (contract RFMEFI61314X0029).

REFERENCES

1. M. Inoue, R. Fujikawa, A. Baryshev, A. Khanikaev, P. Lim, H. Uchida, O. Aktsipetrov, A. Fedyanin, T. Murzina, and A. Granovsky, "Magnetophotonic crystals," *J. Phys. D: Appl. Phys.* **39**(8), p. R151, 2006.
2. K. Nakamura, K. Kudo, T. Goto, H. Takagi, P. Lim, and M. Inoue, "Colorization of magnetic hologram images with optical space division method," *IEEE Trans. Magn.* **50**(11), pp. 1–4, 2014.
3. Y. Nakamura, H. Takagi, P. Lim, and M. Inoue, "Magnetic volumetric hologram memory with magnetic garnet," *Opt. Exp.* **22**(13), pp. 16439–16444, 2014.
4. A. Kirilyuk, A. Kimel, and T. Rasing, "Ultrafast optical manipulation of magnetic order," *Rev. Mod. Phys.* **82**(3), p. 2731, 2010.
5. C. Stanciu, F. Hansteen, A. Kimel, A. Kirilyuk, A. Tsukamoto, A. Itoh, and T. Rasing, "All-optical magnetic recording with circularly polarized light," *Phys. Rev. Lett.* **99**(4), p. 047601, 2007.
6. V. Gasparian, M. Ortuno, J. Ruiz, and E. Cuevas, "Faraday rotation and complex-valued traversal time for classical light waves," *Phys. Rev. Lett.* **75**(12), p. 2312, 1995.
7. G. Airy, "On the intensity of light in the neighbourhood of a caustic," *Camb. Phil. Soc. Trans.* **6**(3), pp. 379–402, 1838.
8. H. Ling, "Theoretical investigation of transmission through a faraday-active fabry-perot etalon," *JOSA A* **11**(2), pp. 754–758, 1994.
9. A. Chetvertukhin, M. Sharipova, A. Zhdanov, T. Shapaeva, T. Dolgova, and A. Fedyanin, "Femtosecond time-resolved Faraday rotation in thin magnetic films and magnetophotonic crystals," *J. Appl. Phys.* **111**(7), p. 07A944, 2012.
10. M. Shcherbakov, P. Vabishchevich, V. Komarova, T. Dolgova, V. Panov, V. Moshchalkov, and A. Fedyanin, "Ultrafast polarization shaping with fano plasmonic crystals," *Phys. Rev. Lett.* **108**(25), p. 253903, 2012.
11. K. Hipps and G. Crosby, "Applications of the photoelastic modulator to polarization spectroscopy," *J. Phys. Chem.* **83**(5), pp. 555–562, 1979.
12. A. Musorin, P. Perepelkin, M. Sharipova, A. Chetvertukhin, T. Dolgova, and A. Fedyanin, "Polarization sensitive correlation spectroscopy of faraday effect femtosecond dynamics," *Bull. RAS. Physics* **78**(1), pp. 43–48, 2014.